Shot noise and electron counting measurements on coupled quantum dot systems

2008 J. Phys.: Condens. Matter 20 454204

(http://iopscience.iop.org/0953-8984/20/45/454204)

IOP PUBLISHING JOURNAL OF PHYSICS: CONDENSED MATTER

J. Phys.: Condens. Matter **20** (2008) 454204 (5pp) doi:10.1088/0953-8984/20/45/454204

Shot noise and electron counting measurements on coupled quantum dot systems

F Hohls, N Maire, C Fricke, M C Rogge and R J Haug

Institut für Festkörperphysik, Leibniz Universität Hannover, Appelstraße 2, 30167 Hannover, Germany

E-mail: hohls@nano.uni-hannover.de

Received 8 May 2008
Published 23 October 2008
Online at stacks.iop.org/JPhysCM/20/454204

Abstract

Measuring shot noise and electron counting are both methods for accessing information about the dynamics of electronic transport through a system of interest. Here we apply these tools to examine electronic transport through coupled quantum dot systems. In the first part of the paper we show temperature dependent shot noise measurements for a strongly coupled double-quantum-dot system. We observe super-Poissonian shot noise as expected for coherent inter-dot coupling and asymmetric lead tunnelling rates. In the second part we apply direct electron counting to examine a weakly coupled triple-dot system. A quantum point contact placed near the triple dot allows us to monitor electron hops between the dots and the leads. This allows us to, e.g., individually characterize different tunnelling rates relevant in the system.

(Some figures in this article are in colour only in the electronic version)

1. Introduction

Coupled quantum dot systems allow us to study quantum mechanical effects in a well controlled model system and also offer interesting prospects as building blocks for quantum information processing. The present understanding of such systems is mainly based on direct current transport experiments; see e.g. [1] for double dots. But a wealth of additional information can be gained from shot noise measurements on mesoscopic systems as was nicely pointed by Blanter and Büttiker in their classic review [2]. We will use such measurements in the first part of this paper to characterize a double-quantum-dot system, revealing the coherent nature of the coupling between the quantum dots.

The measurement of shot noise is only possible for sufficiently large current, i.e. sufficiently large rates of tunnelling between the dot system and the leads. However, for applications in quantum information processing the quantum dot system has to be set to low tunnelling rates. Direct current shot noise measurements are not possible in this regime. Instead one can characterize such systems using a quantum point contact (QPC) placed nearby as a charge detector [3]. If the measurement bandwidth of this detector exceeds the relevant tunnelling times within the quantum dot systems, one can realize a real time detection of electron tunnelling events [4–6]. We will use this technique in the second part of this paper to characterize a triple-quantum-dot system in the regime of low tunnelling rates.

2. Shot noise measurements for a coupled quantum dot system

Electrical shot noise was first discussed by Schottky who examined noise sources in vacuum tubes [7]. His result for the low frequency noise power of the current, $S_P = 2eI$, is valid for any process with Poissonian statistic, e.g. tunnelling of electrons through a thick barrier, and is referred to as the full Poissonian shot noise. For resonant tunnelling through a double-barrier system one expects a reduced shot noise. The amount of noise reduction is characterized by the Fano factor, $\alpha = S/(2eI)$, with S the observed noise power spectral density. For resonant tunnelling through the ground state of a single quantum dot, sequential [8] and coherent [9] tunnelling calculations predict the same suppressed value of the Fano factor. The predicted noise reduction was experimentally

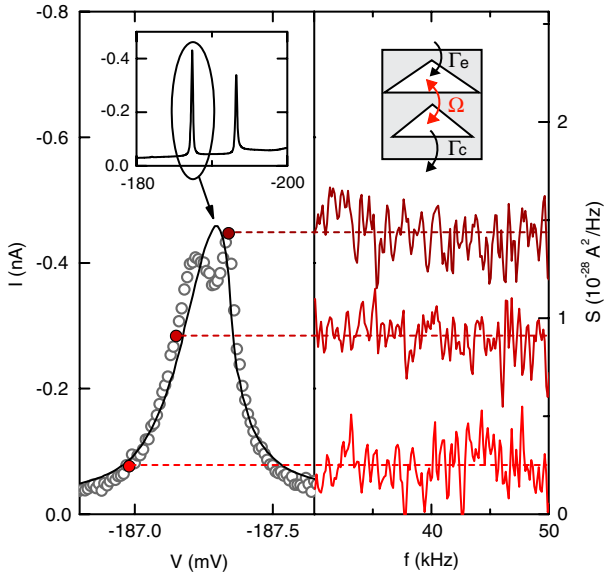

Figure 1. Left: voltage dependence of the current (line, left axis) and the shot noise (circles, right axis) for resonant electron tunnelling through a double-quantum-dot stack. Right: shot noise spectra for different voltage positions marked by the filled circles in the left part. Inset: schematic diagram of the quantum dot stack.

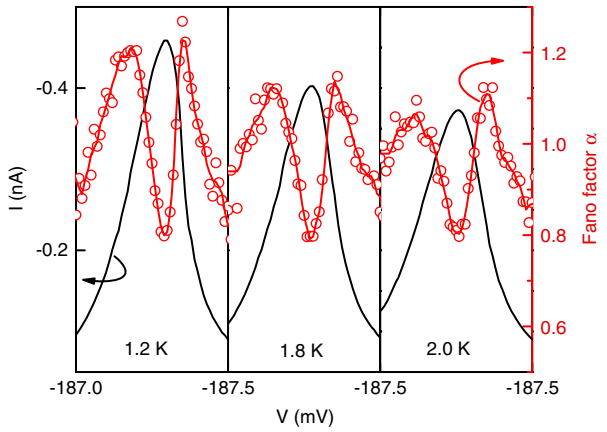

Figure 2. Voltage dependence of the current (black line, right axis) and Fano factor (circles, right axis) for different temperatures. The line passing through the circles is the result of a five-point average.

confirmed for single quantum dots with good quantitative agreement [10, 11].

Motivated by these results we have extended the shot noise measurements to in series coupled double-dot systems. We use self-organized InAs dots in AlAs tunnelling barriers with GaAs leads. For details of the device see [12, 13]. The noise measurements were performed using the technique already described in [10, 11, 13].

The right inset in figure 1 displays a schematic diagram of the double-dot system. The leads above and below are not shown. For transport measurements a large bias is applied across the device. This ensures that the tunnelling from the emitter lead into the dot system (rate Γ_e) and also the tunnelling from the dots into the collector (rate Γ_c) are both unidirectional as all accessible emitter states are occupied and all collector states are empty. However tunnelling between the quantum dots (rate Ω) can happen in both directions if the dots are aligned. The rates are asymmetric for the chosen device geometry, $\Gamma_e \sim \Omega \gg \Gamma_c$.

Due to the growth parameters, the two quantum dots have different size and therefore different ground state energies. When applying a voltage V across the device the energies of both dots are shifted with respect to the emitter with different lever arms. This allows us to bring them in and out of resonance by simply changing V. A large resonant current is observed when the two dots are in resonance [12, 13]. The left of figure 1 shows a blow-up of the current resonance for a selected quantum dot stack. We have measured the noise spectra $S(f)$ for different voltages throughout the current peak and determined the shot noise power S by averaging over the frequency range $f = 30$–50 kHz. The result is shown by the circles. Already the unscaled noise power S shows a behaviour that differs from that of the current: instead of a single resonance peak we observe a double-peak behaviour.

Now we will discuss the Fano factor $\alpha = S/2eI$. Figure 2 displays the voltage dependence of the Fano factor in comparison to the current for different temperatures. The first point to notice is the occurrence of super-Poissonian noise ($\alpha > 1$) [13]. At first glance this might come as a surprise: calculations for sequential tunnelling through a double-dot system with a strong Coulomb blockade as given in our device found a sub-Poissonian value $\alpha < 1$ under all circumstances. But the theoretical prediction changes when taking a coherent coupling between the dots into account: the calculation in [14] reproduces both the enhanced noise with $\alpha > 1$ and its double-peak structure for asymmetric rates $\Gamma_e \sim \Omega \gg \Gamma_c$. Even the temperature dependence is well accounted for: the coupling to the phonon bath leads to decoherence which increases with rising temperature and thereby reduces/suppresses the super-Poissonian noise at elevated temperatures.

In the following we want to give a illustrative reasoning for the occurrence of super-Poissonian noise for coherently coupled quantum dots: at the resonance of the quantum dot ground states two molecular states are formed. For exact alignment the two molecular states have an equal weight distribution across both quantum dots; the resonant current is maximal and it is distributed equally on the two quantum dots. The Fano factor is the one of simple resonant tunnelling, i.e. $\alpha \leqslant 1$. The molecular states also persist to slightly larger or smaller voltage where the quantum dot states are slightly detuned. However, the weight of the molecular wavefunction is shifted towards the one dot for the first state and towards the other dot for the second molecular state. Now two unequal resonant current paths with unequal coupling to the leads exist. Due to the strong Coulomb blockade it is forbidden to occupy both states. In this situation the state with the larger weight near the emitter has a lower collector tunnelling rate Γ_c^1. If an electron tunnels into this state, it blocks the current through the second channel. The current is mainly determined by the collector tunnelling rate since $\Gamma_e \gg \Gamma_c$. Therefore the second state with $\Gamma_c^2 > \Gamma_c^1$ is the main current carrying state. The

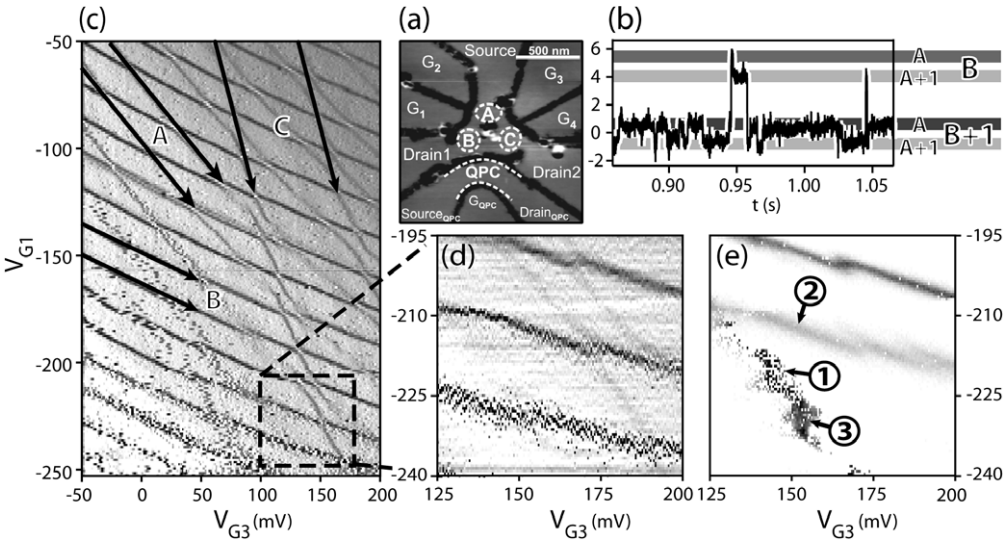

Figure 3. (a) AFM micrograph of the device showing the triple-dot system (quantum dots A, B, C) and the nearby quantum point contact (QPC) acting as a charge detector. (b) Time trace of the charge signal at position (3) in figure panel (e) (arbitrary units and offset). A and A + 1 denote electron number states of dot A, B and B + 1 those of dot B. (c) Charging diagram of the triple-dot system; see panel (a) for the position of the G_1 and G_3 gates (no applied source–drain voltage). The displayed signal is dI_{qpc}/dV_{G3}. The arrows marked A, B and C mark the different slopes of charging lines for different dots. (d) Charging measurement with increased gate voltage resolution. The equivalent gate voltage range is marked by the square in panel (c). The slight voltage offset is probably caused by a trapped charge. (e) Number of counting events detected by the charge detector for the same gate voltage range.

recurrent blocking of the fast second transport channel due to the first slow channel leads to electron bunching and thereby to super-Poissonian noise $\alpha > 1$ as was shown theoretically for a two-channel resonant tunnelling system with strong Coulomb blockade in [8].

We can also understand the temperature dependence within this picture: transitions between the blocking molecular state and the transport state at detuned resonance can be mediated by phonons. Phonon absorption depends on the occupation of phonon states at nonzero temperature and therefore rises with rising temperature. Spontaneous phonon emission is possible at zero temperature, but at $T > 0$ stimulated emission due to thermal phonons increases the rate of this inelastic process. Thus for both positive and negative detuning, i.e. for both sides of the current peak, we expect a less pronounced noise enhancement at rising temperatures and finally at elevated temperatures even $\alpha < 1$.

In summary for the first part of the paper, we have shown noise measurements for a coupled quantum dot system. The observed super-Poissonian shot noise reveals the coherent nature of the inter-dot coupling.

3. Electron counting for a triple quantum dot

Now we will focus on an electron counting experiment performed for a triple quantum dot. The device was fabricated by AFM oxidization of an AlGaAs/GaAs heterostructure. Figure 3(a) displays an AFM micrograph of the triple-dot system with nearby QPC charge detector. A detailed description and characterization of this device are given in [15]. In this paper we will concentrate on charge detection measurements. All measurements were performed in a dilution refrigerator with base temperature $T < 0.1$ K. All lead potentials are set to zero within the accuracy of the offset compensation ($\sim$10 μV) of the current amplifiers attached to the drain leads.

Figure 3(c) displays the charging diagram of the triple-quantum-dot system for variation of the two gates G_1 and G_3. Devices patterned by AFM lithography are well suited for sensitive charge detection [6, 16, 17] due to the absence of metal gates which would partially screen the coupling between the dots and the charge detector. This allows us not only to detect charge state transitions in the dots B and C near the QPC but also those of dot A. This is revealed by the observation of lines with three different slopes in figure 3(c). The slopes are directly related to the ratio of the geometrical distances between each dot and the gates G_1 and G_3. This allows a unique assignment between a charging line and the charged quantum dot.

The gates voltages not only change the electron number on the quantum dots but also alter the rates of tunnelling between the dots and the leads. This becomes apparent in the lower part of figure 3(c) where the lines dissolve into dots. Here the tunnelling rates become comparable to the data taking period. This control of the tunnelling rate allows us to choose a range where we can resolve individual tunnelling events in a time dependent measurement. Figure 3(d) shows a high resolution measurement of the regime of interest for counting experiments.

Figure 3(b) shows a time dependent trace of the charge detector signal for certain gate voltages. One can distinguish four different levels which are related to different charge configurations of quantum dot A and B. Charging of quantum dot B gives a rather large step as it is very near to the charge detector; the step for the addition of one electron to dot A

is smaller due to the larger distance but can still be resolved. Similar measurements for individual quantum dots were used to experimentally access the full counting statistics [18, 19].

The ability to resolve individual charging events on the dots gives us information complementary to the change of the average charge as measured by the DC signal of the QPC which was plotted in figures 3(c) and (d). In figure 3(e) the number of charging events per second, i.e. the average charge transition rate, is plotted for the same gate voltage range as was used in figure 3(d).

Now we will demonstrate the use of real time counting for a characterization of our device. First we choose a gate voltage set such that quantum dot A is in resonance with the source lead. This position is marked as (1) in figure 3(e). We now measure the time after each A+1 $\rightarrow$ A transition until the next A $\rightarrow$ A + 1 transition occurs, i.e. the time to add an electron onto dot A. We then bin all measured times into a distribution $N_{\mathrm{in}}(\tau)$ as plotted in figure 4(a). The distribution can now be fitted by an exponential decay, $N_{\mathrm{in}}(\tau) \propto \exp[-\Gamma_{\mathrm{in}}\tau]$, to derive the rate Γ_{in} for tunnelling from the source lead onto dot A. The same procedure, now for the times between the A $\rightarrow$ A + 1 and the A + 1 $\rightarrow$ A transitions, allows us to determine the rate Γ_{out}, out of the dot onto the lead. For this special gate voltage choice we find $\Gamma_{\mathrm{in}} = 154$ Hz $< \Gamma_{\mathrm{out}} = 251$ Hz. The imbalance towards Γ_{out} reveals that the chemical potential of the quantum dot E_{d} at this gate voltage setting is larger than the Fermi energy E_{F} of the lead and therefore $f(E_{\mathrm{d}}) < 0.5$ ($f(E)$ is the Fermi distribution).

We can perform the same procedure to determine rates of tunnelling between dot B and the 'drain1' lead. We choose a gate voltage position on the charging line for dot B in figure 3(e) marked by (2); for this position the other quantum dots are off resonance. The result of the analysis is displayed in figure 4(b). Here $\Gamma_{\mathrm{in}} = 58$ Hz $> \Gamma_{\mathrm{out}} = 29$ Hz and therefore E_{d} is slightly below E_{F}. The rates for dot C are too low in this gate voltage range to gather a sufficient amount of events for such an analysis.

We have now demonstrated how to characterize the tunnelling rates in such a system. In this analysis we concentrated on the resonance between one of the dots and its adjacent lead. Next we will briefly focus on a so called triple point where two quantum dots are in resonance with their leads and with each other. This happens e.g. at point (3) in figure 3(e). We should recall that the source–drain bias voltage is zero. In this situation electrons can traverse the quantum dots from one lead to the other one due to the finite width of the Fermi distribution. Figure 4(c) displays a time segment that shows such a process: an electron tunnels from drain1 onto dot B and then onto dot A and finally leaves dot A into the source. As demonstrated by Fujisawa *et al* [20] this allows e.g. a bidirectional current measurement at very low currents even when the bias voltage does not impose a definite direction on the electrons.

It is very interesting to note that before the electron leaves dot A to go into the lead, an additional electron enters dot B. This should be forbidden by Coulomb blockade—for zero source–drain bias no electrons should have sufficient energy. But this assumption neglects an additional source of energy:

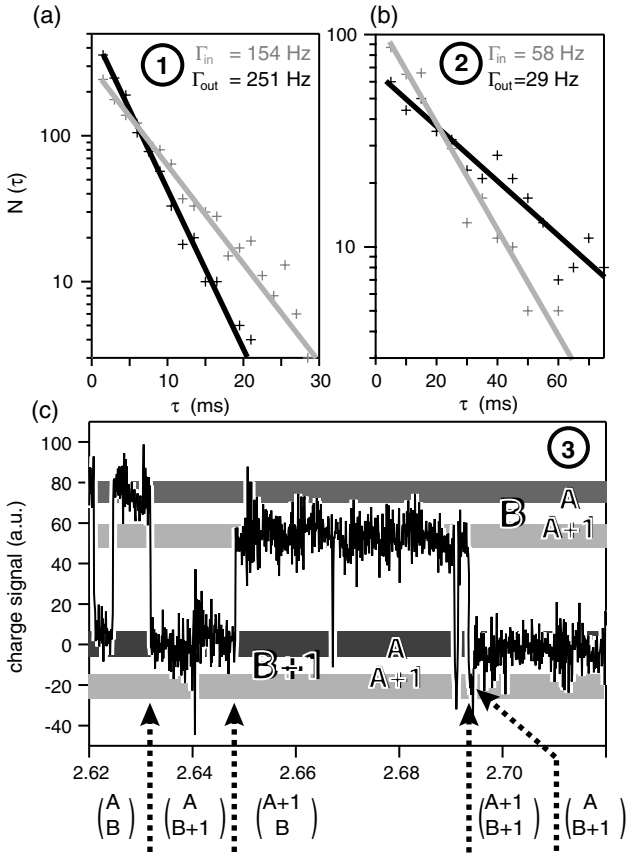

Figure 4. (a) Tunnelling rate distribution $N(\tau)$ at position (1) in figure 3(e) for tunnelling onto (Γ_{in}) and off (Γ_{out}) dot A from and to the source lead. The lines show exponential fits of $N(\tau) \propto \exp[-\Gamma\tau]$. (b) Same for dot B and lead 'drain1', measured at position (2) in figure 3(e). (c) Time trace of charge detector signal (arbitrary units and offset) at position (3) in figure 3(e) (horizontal axis: time in seconds). The trace shows transport of one electron from drain1 via dot B and dot A to the source.

the quantum point contact is biased with 4 mV. It was shown before that this can lead to hot electrons in the leads; see e.g. [21].

We could not yet observe three-dot counting at a quadruple points due to a too large imbalance of the tunnelling rates. This will be one of the goals for future measurements.

4. Summary

In this paper we have demonstrated the exemplary use of noise measurements and real time electron counting for the characterization of multi-dot systems. In the first part we have shown temperature dependent shot noise measurements for a double quantum dot. We observe super-Poissonian noise that reveals the coherent nature of the inter-dot coupling. The shot noise is reduced for enhanced temperature due to an increased rate of inelastic processes. In the second part we have presented real time electron counting results for a triple-dot system. We have characterized the system in a regime of low tunnelling rates and demonstrated bidirectional transport measurement for zero bias voltage.

Acknowledgments

We acknowledge K Pierz (PTB Braunschweig) for the MBE growth of the InAs quantum dot systems used for the shot noise experiments. W Wegscheider (Universität Regengsburg), M Bichler and G Abstreiter (WSI Munich) supplied the heterostructure used to manufacture the triple-dot system.

The explanation of the observed super-Poissonian shot noise was developed in collaboration with G Kießlich and E Schöll (Technische Universität Berlin).

The work was mainly funded by the BMBF within the nanoQUIT programme.

We would also like to thank G Bauer (Universität Linz) for his commitment to the nanoQUIT programme and his helpful suggestions as regards our projects within this programme.

References

[1] van der Wiel W G, De Franceschi S, Elzerman J M, Fujisawa T, Tarucha S and Kouwenhoven L P 2002 *Rev. Mod. Phys.* **75** 1
[2] Blanter Y M and Buttiker M 2000 *Phys. Rep.* **336** 1–166
[3] Field M, Smith C G, Pepper M, Ritchie D A, Frost J E F, Jones G A C and Hasko D G 1993 *Phys. Rev. Lett.* **70** 1311
[4] Elzerman J M, Hanson R, Willems van Beveren L H, Witkamp B, Vandersypen L M K and Kouwenhoven L P 2004 *Nature* **430** 431
[5] Fujisawa T, Hayashi T, Hirayama Y, Cheong H D and Jeong Y H 2004 *Appl. Phys. Lett.* **84** 2343
[6] Schleser R, Ruh E, Ihn T, Ensslin K, Driscoll D C and Gossard A C 2004 *Appl. Phys. Lett.* **85** 2005
[7] Schottky W 1918 *Ann. Phys.* **57** 541
[8] Kiesslich G, Wacker A and Scholl E 2003 *Phys. Rev.* B **68** 125320
[9] Thielmann A, Hettler M H, Konig J and Schon G 2003 *Phys. Rev.* B **68** 115105
[10] Nauen A, Hapke-Wurst I, Hohls F, Zeitler U, Haug R J and Pierz K 2002 *Phys. Rev.* B **66** 161303R
[11] Nauen A, Hohls F, Maire N, Pierz K and Haug R J 2004 *Phys. Rev.* B **70** 033305
[12] Sarkar D, Zeitler U, Hapke-Wurst I, Haug R J and Pierz K 2003 Tunnelling through vertically coupled InAs quantum dots *Physics of Semiconductors—26th ICPS (Edinburgh 2002)* (*Inst. Phys. Conf. Ser.* vol 171) ed A R Long and J H Davies (Beograd: Institute of Physics Publishing)
[13] Barthold P, Hohls F, Maire N, Pierz K and Haug R J 2006 *Phys. Rev. Lett.* **96** 246804
[14] Kiesslich G, Scholl E, Brandes T, Hohls F and Haug R J 2007 *Phys. Rev. Lett.* **99** 206602
[15] Rogge M C and Haug R J 2008 *Phys. Rev.* B **77** 193306
[16] Fricke C, Rogge M C, Harke B, Reinwald M, Wegscheider W, Hohls F and Haug R J 2005 *Phys. Rev.* B **72** 193302
[17] Rogge M C, Harke B, Fricke C, Hohls F, Reinwald M, Wegscheider W and Haug R J 2005 *Phys. Rev.* B **72** 233402
[18] Gustavsson S, Leturcq R, Simovic B, Schleser R, Ihn T, Studerus P, Ensslin K, Driscoll D C and Gossard A C 2006 *Phys. Rev. Lett.* **96** 076605
[19] Fricke C, Hohls F, Wegscheider W and Haug R J 2007 *Phys. Rev.* B **76** 155307
[20] Fujisawa T, Hayashi T, Tomita R and Hirayama Y 2006 *Science* **312** 1634
[21] Khrapai V S, Ludwig S, Kotthaus J P, Tranitz H P and Wegscheider W 2007 *Phys. Rev. Lett.* **99** 096803